ACS SENSORS

pubs.acs.org/acssensors Article

High-Throughput Strategy for Enhancing Aptamer Performance across Different Environmental Conditions

Leighton Wan, Alex Yoshikawa, Michael Eisenstein, and H. Tom Soh*

Cite This: https://doi.org/10.1021/acssensors.2c02106 Read Online

ACCESS | Metrics & More | Article Recommendations | Supporting Information

ABSTRACT: Aptamers selected under specific environmental conditions (e.g., pH, ion concentration, and temperature) often exhibit greatly reduced affinity when used in other contexts. This can be especially problematic for biomedical applications in which aptamers are exposed to sample matrices with distinctive chemical properties, such as blood, sweat, or urine. We present a high-throughput screening procedure for adapting existing aptamers for use in samples whose chemical composition differs considerably from the original selection conditions. Building on prior work from our group, we have utilized a modified DNA sequencer capable of screening up to 10^7 unique aptamer mutants for target binding under the desired assay conditions. As an exemplar, we screened all 11,628 single- and double-substitution mutants for a previously reported glucose aptamer that was originally selected in high-ionic strength buffer and exhibited relatively low affinity in physiological conditions. After a single round of screening, we identified aptamer mutants with ~four-fold increased affinity in physiological conditions. Interestingly, we found that the impact of single-base substitutions was relatively modest but observed considerably greater binding improvements among the double mutants, highlighting the importance of cooperative effects between mutations. This approach should be generalizable to other aptamers and environmental conditions for a range of applications.

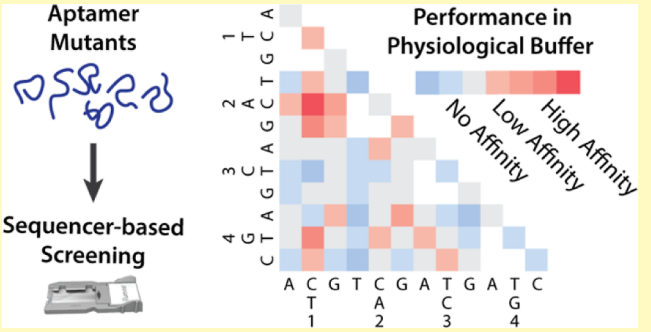

KEYWORDS: *aptamers, high-throughput screening, structure-switching, physiological, biosensors*

INTRODUCTION

Aptamers are nucleic acid-based affinity reagents that are generated based on their target-binding properties through in vitro screening using systematic evolution of ligands by exponential enrichment (SELEX).[1,2] These selection protocols are typically designed to generate an enriched aptamer pool that exhibits high affinity against a target in a defined set of environmental conditions such as the pH, ion concentration, and temperature. As a consequence, aptamers often exhibit greatly reduced binding performance when used in conditions that are notably different than those used during selection.[3,4] For example, the concentration of divalent cations such as Mg^{2+} is crucial for the formation of aptamer tertiary structure, including binding pockets responsible for target recognition.[5−8] In another example, an aptamer that binds tetracycline with high affinity in the presence of Mg^{2+} loses its ability to bind this target in the absence of magnesium.[5] pH and Na^+ ion concentrations can likewise influence ligand binding through mechanisms such as protonation of aptamer-binding sites. A cocaine-binding aptamer that exhibited an optimal K_D at pH 7.4 lost binding function at pH 9.6, along with a 20-fold reduction in affinity at increased NaCl concentrations.[9] This becomes a critically important consideration in the context of real-world applications such as molecular diagnostics. A high-quality aptamer selected in a particular buffer may lose affinity or specificity when used in clinically relevant specimens with chemical properties that differ meaningfully from that buffer, such as blood, sweat, or urine, requiring the identification of new aptamers that perform well in the desired conditions.

We describe here a high-throughput mutational screening procedure for adapting existing aptamers for use in assay conditions that differ from those used in the initial selection. This strategy employs our previously published non-natural aptamer array (N2A2) platform,[10,11] making use of a modified Illumina MiSeq instrument to screen the binding properties of vast pools of single- and double-substitution mutants of the parent aptamer sequence. As a proof of concept, we applied this approach to a previously published glucose aptamer, which exhibits an equilibrium dissociation constant (K_D) of 10 mM when used in the high-salt HEPES-based buffer employed in the original SELEX process.[12] We found that this aptamer exhibits a

Received: September 26, 2022
Accepted: May 30, 2023

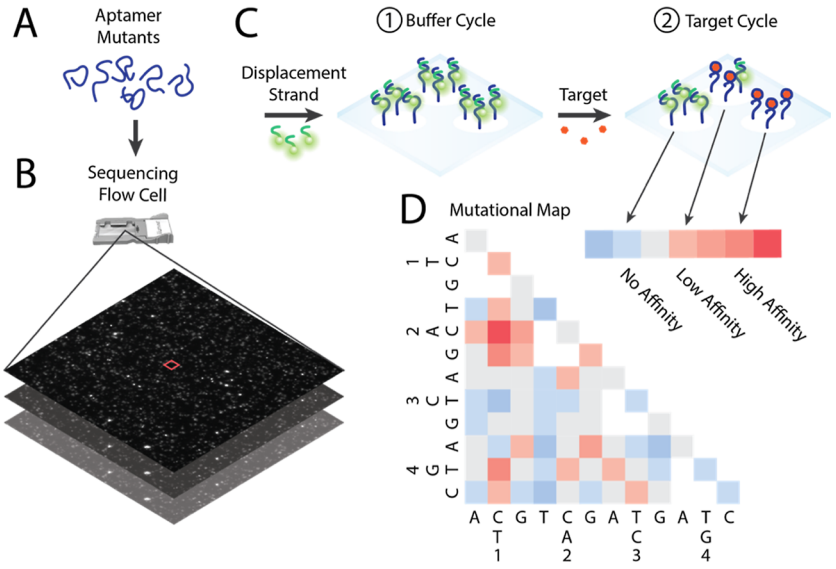

Figure 1. Workflow for the high-throughput screen of aptamer mutants for binding optimization in new buffer. (A) Aptamer mutants are converted to aptamer clusters and then screened using a modified Illumina sequencer and (B) flow cell. (C) Screening is performed using alternating "buffer" and "target" cycles. During buffer cycles, a Cy3-labeled displacement strand is added, washed in selection buffer, and then the clusters are imaged. During target cycles, 100 mM target in the same buffer is added, followed by washing and imaging. The process is repeated for both the original and desired selection buffer. (D) High-throughput screening data is then used to generate a mutational map from which candidate sequences are chosen for further characterization.

nearly 10-fold higher K_D (i.e., lower affinity) at physiological salt concentrations, and this would make it less useful for detecting physiological concentrations of blood glucose, which typically range between 5.6 mM during fasting and 7.8 mM after eating in healthy individuals.[13] Using our platform, we were able to discover mutant versions of this aptamer that exhibit nearly fourfold improved affinity for glucose in these lower-salt conditions, offering a better match for physiological applications. Since our platform enables comprehensive screening of single- and double-mutant libraries for a given aptamer, we were also able to identify key structural features of the aptamer that could offer fruitful targets for further engineering and functional optimization of the aptamer sequence.

RESULTS

Design of the High-Throughput Mutant Screening Process. We used our N2A2 platform as a means for comprehensively surveying the structure and function of the full landscape of single and double mutants for our glucose aptamer (glu0), which was initially isolated by Nakatsuka et al.[12] N2A2 is based on a modified Illumina Miseq sequencing instrument, which performs both high-throughput sequencing and screening of aptamer clusters on the flow-cell surface. The MiSeq flow cell can accommodate as many as 10^7 aptamer clusters, which is more than sufficient to achieve full coverage of the single- and double-mutant space for most existing aptamers in a single experiment—for example, the sequence space of single- and double-substitution mutations for an 80-mer aptamer consists of 28,681 sequences. Microarray-based screening is an alternative approach well suited for short aptamer sequences with fewer mutants.

The canonical first read of the high-throughput sequencing run is used to generate and sequence the aptamer clusters (Figure 1A). Instead of a traditional second, paired-end read, the N2A2 then measures the fluorescence of the aptamer clusters, which is produced through the hybridization of a fluorescently labeled, complementary displacement strand. This strand is displaced when the aptamers at a given cluster bind to the target molecule, providing a measurable readout of binding activity. This activity is measured in alternating "buffer" and "target" cycles (Figure 1B). During the buffer cycle, the fluorescently labeled displacement strand is annealed to aptamer clusters, washed with buffer, and then imaged to measure the affinity for the displacement strand. In the following target cycle, the flow cell is incubated with the target (i.e., glucose) in buffer and then washed and imaged in order to measure the extent to which the displacement strand signal is reduced relative to the buffer cycle (Figure 1C). A large relative difference indicates a greater response to the target, presumably due to binding-induced strand displacement, whereas a smaller or no fluorescence change generally indicates aptamers that have minimal target binding activity. In this fashion, the relative degree of aptamer binding to targets can be measured while linking this binding performance directly to the relevant aptamer cluster sequence. Finally, the response to target can be used to generate a mutation map to investigate aptamer function and sequence elements that can potentially be targeted to achieve improved binding performance (Figure 1D).

Mutational Screen of Glucose Aptamer Response in Physiological Conditions. The glu0 aptamer tested here was originally selected in a high-ionic-strength (1.035 M) HEPES buffer and exhibited a K_D of 10 mM in this buffer. However, we found that its affinity is greatly reduced in our selection buffer (20 mM Tris−HCl, 120 mM NaCl, 5 mM KCl, 1 mM $MgCl_2$, 1 mM $CaCl_2$, and 0.01% Tween 20), which more closely mirrors physiological conditions with an ionic strength of 144 mM. We measured the aptamer's K_D in both HEPES buffer and selection buffer using the same plate-reader assay used in the original paper.[12,14] Briefly, this assay measures the K_D of the aptamer as the ratio of the aptamer's affinity for a displacement strand ($K_{D,1}$) relative to the response of the aptamer-displacement strand complex to the target ($K_{D,2}$) (Figure S1A). The

https://doi.org/10.1021/acssensors.2c02106
ACS Sens. XXXX, XXX, XXX−XXX

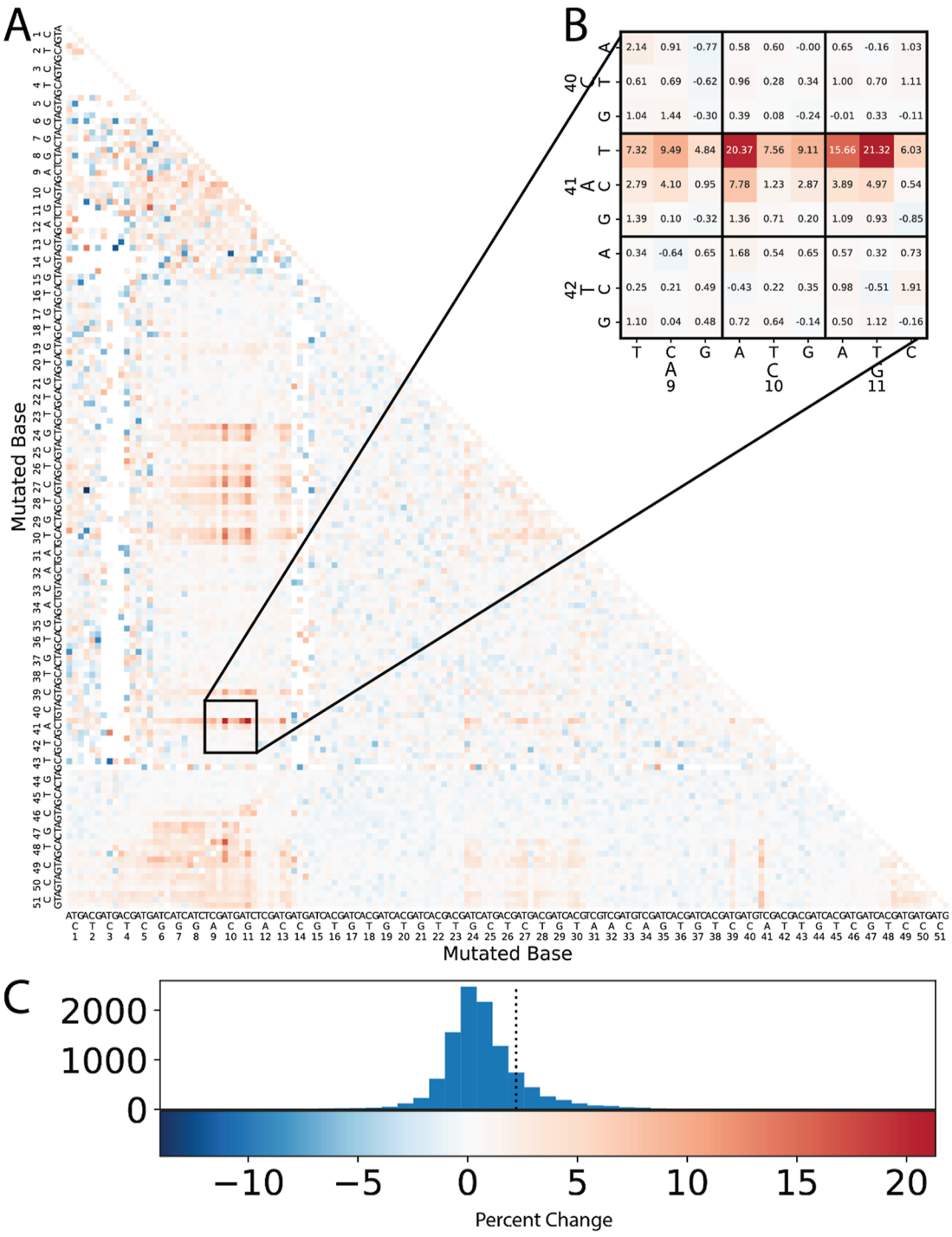

Figure 2. Heatmap of glucose binding by glu0 single and double mutants. (A) Full sequence map shows all sequences that passed filtering. Colors depict mean normalized percent change values, wherein the percent change observed for a given sequence in selection buffer alone was subtracted from the percent change observed with glucose. Sequences with a large positive percent change are shown in red, while sequences with a negative percent change are shown in blue. Sequences removed in filtering are shown in white (8% of sequences). The labels on each axis show the mutant position in the sequence, original base, and the base substitution. For example, mutations at the first position are from the original cytosine, and to adenine, thymine, or guanine. (B) Magnification of a portion of the heatmap containing the candidate sequences with the highest percent changes. The legend for the heatmap in A and B is shown at bottom. (C) Distribution of percent changes for all mutants is shown as a histogram, with the percent change for parent aptamer glu0 marked as a dotted line.

displacement strand sequence was based on that from the original paper (Table S1). Based on this assay, we measured a K_D of 3.65 ± 0.59 mM in HEPES buffer versus 90.5 ± 7.6 mM in selection buffer (Figure 1B,C). As such, this aptamer would be of limited use for measuring physiological levels of glucose in blood, which range from <5.6 mM during fasting and up to 7.8 mM after eating in healthy individuals and are greater in diabetic patients.[13]

In order to profile the binding of various aptamer mutants in our selection buffer, we generated a pool of 11,628 single and

https://doi.org/10.1021/acssensors.2c02106
ACS Sens. XXXX, XXX, XXX−XXX

double mutants based on the 51-mer glu0 sequence. We created a comprehensive list of mutants by substituting the base at one to two positions to cover all single and double substitution mutants (11,628 total). We then ordered the single- and double-mutant pool from TWIST Biosciences. The pool was then indexed and prepared for high-throughput sequencing and screening. During buffer cycles, we measured aptamer cluster binding to a Cy3-labeled 15-mer displacement strand (Table S1). In the subsequent target cycles, we introduced either 100 mM glucose or target-free buffer as a control, and once again measured fluorescence. We chose a stringent concentration of 100 mM glucose to accommodate competition with the displacement strand. This is well above the measured K_D for glu0 in both selection buffer and HEPES and should thus readily reveal aptamer variants with superior binding properties. We then processed the sequence-intensity data by filtering out outliers and artifacts and removing sequences with <5 replicates to minimize the impact from experimental noise (see Supporting Information for details). To control for greater displacement of the Cy3-labeled strand in the absence of target, we normalized our measurements by subtracting the percent change in target-free control cycles from the percent change in 100 mM glucose cycles. Hereafter, "percent change" in response to glucose refers to this normalized measurement.

We measured a total of 3.7 million aptamer clusters to identify aptamers with improved affinity for glucose in selection buffer. After filtering, the screened sequences covered 92.0% of the single- and double-mutant sequence space, with an average of 162 replicate clusters per sequence. We then mapped the mean percent change of each mutant (based on all replicate clusters) onto single- and double-mutant heatmaps to identify mutants that outperformed the parent glucose aptamer (Figure 2A,B). Sequences that had minimal or no function would have negative or near-zero percent changes, whereas mutants that retained affinity would have positive percent changes. Overall, 64.5% of the mutants had positive mean percent changes, and 17.4% exhibited a greater mean percent change than that of the base glucose aptamer (2 ± 15%; Figure 2C). Among the single mutants, 20.3% of sequences outperformed the base glucose aptamer (glu0) versus 17.3% for the various double mutants, and we subsequently embarked on a closer examination of the effects of specific mutations.

Characterizing the Functional Impact of Individual Aptamer Mutations. The high-throughput mutational screen provided insight on specific mutations that influence glucose binding. We categorized the single mutants with a mean percent change greater than glu0 into four groups: the displacement strand-binding domain of the aptamer (bases 1−15), the "stem-forming" sequence complementary to part of this domain (bases 44−51), the A41T mutant within the aptamer's large primary loop and in a hairpin loop domain (bases 24−30) (Figure 3A). Mutations in the displacement strand-binding region of the aptamer are expected to destabilize hybridization with both the displacement strand and the formation of the stem at the end of the aptamer. In contrast, mutations in the complementary stem-forming domain at the end of the aptamer are expected to only destabilize the stem, shifting equilibrium in favor of the aptamer remaining bound to the displacement strand. The single mutants with the highest percent changes were C10A and G11T, with percent changes of 7 ± 15 and 7 ± 17%, respectively. These alterations fell within the displacement strand-binding domain, and other highly ranked single-substitution sequences also affected this same domain.

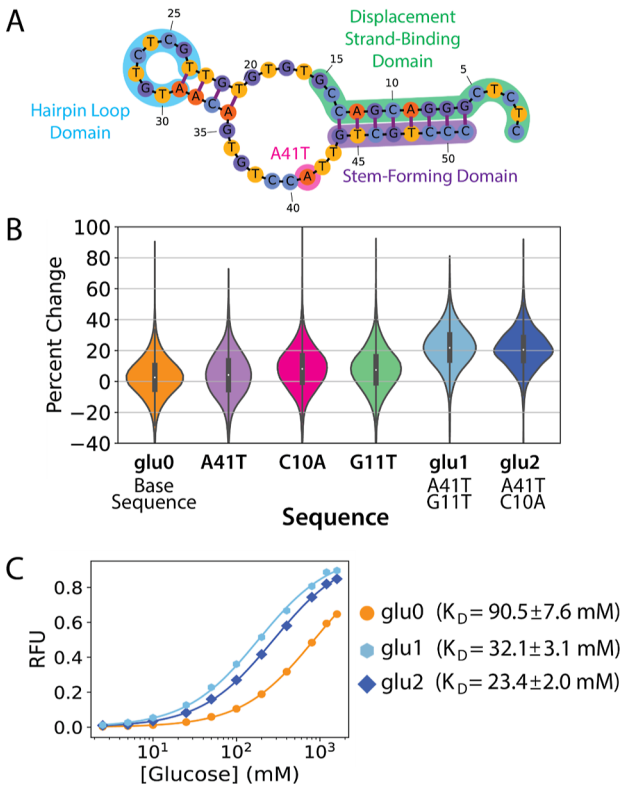

Figure 3. Characterization of high-performing aptamer mutants. (A) Secondary structure of glu0 as predicted by NUPACK.[15] Four domains are highlighted: the displacement strand-binding domain (green), the hairpin loop (blue), the A41T mutation (magenta), and the stem-forming domain (purple). (B) Violin plots for the percent changes for the glu0 base sequence and for mutants A41T, C10A, G11T, glu1 (A41T/G11T), and glu2 (A41T/C10A). The thick, dark bar in the center of the violin plot shows the interquartile range, and the white dots mark the median percent change. The profile of each "violin" shows a density plot of percent changes measured in the N2A2 assay. (C) Plot shows $K_{D,2}$ measurements for glu0, glu1, and glu2 in selection buffer with a plate-reader assay. We determined the K_D values shown at right based on the ratio of $K_{D,1}$ (data in Figure S4C) and the $K_{D,2}$ values measured here. The points represent the mean, and the bars represent the standard deviation of three measurements.

Although the impact of single substitutions was relatively modest, we observed considerably greater binding improvements in some of our double mutants, highlighting the importance of cooperative effects between mutations. To identify synergistic mutations, we grouped double mutants containing a common single mutation and counted the total number of those mutants with a mean percent change greater than glu0 (Figure S2). The group containing the A41T substitution had the greatest number of double mutants outperforming glu0 (64 sequences), followed by the T30C, C10A, and G24A substitution groups, with 60, 60, and 57 sequences, respectively. Our two highest-performing sequences, A41T/G11T (glu1) and A41T/C10A (glu2), showed percent changes of 21 ± 15 and 20 ± 13%, nearly three times greater than the highest-performing single mutant (Figure 3B). Furthermore, we used the two-sample z-test to examine the likelihood of increased percent change over the base glucose sequence. We calculated the two-sample z-test statistics for glu0 with glu1 and glu2 and found the values to be −43.9 and −50.7, respectively. Thus, we are able to reject the null hypothesis with

https://doi.org/10.1021/acssensors.2c02106
ACS Sens. XXXX, XXX, XXX−XXX

high certainty and show that glu1 and glu2 had increased percent changes.

In contrast, while the G24A and T30C groups had high numbers of outperforming mutants, these two mutations did not show synergistic improvements to affinity in combination with other mutants. Individually, the G24A and T30C mutations had low percent changes of 3 ± 15 and 3 ± 17%, respectively, with no notable improvement in affinity (Figure 3A−C). The T30C/A41T mutant also showed no meaningful cooperativity, with a low percent change of 6 ± 21% and minimal improvement to affinity. In terms of secondary structures, the G24A and T30C mutations are predicted to stabilize the stem preceding the hairpin loop, leading to no meaningful impact on glucose binding (Figure S3D). Since the cooperative effects of mutations cannot currently be determined *a priori*, this high-throughput screening procedure becomes invaluable for systematically investigating how to improve the glucose aptamer through multiple mutations and uncovering structural features that contribute meaningfully to ligand-binding.

Characterizing Mutants with Improved Glucose Response in Physiological Conditions. We picked the top-performing double-mutant aptamer candidates, glu1 and glu2, for further validation. We used our plate-reader assay to determine the K_D as a ratio of $K_{D,1}$ and $K_{D,2}$. Increased fluorescence was measured for a Cy3-labeled 14-mer control strand (Table S1) at higher concentrations of glucose (Figure S4A), and we used these background measurements to normalize the measured fluorescence observed from the aptamers with glucose at the same concentrations (Figure S4B). The calculated K_D values for glu1 and glu2 were 32.1 ± 3.1 and 23.4 ± 2.0 mM, respectively, versus 90.5 ± 7.6 mM for glu0 in selection buffer (Figure 3C and Figure S4C), representing a ∼3−4-fold change improvement. This improved K_D in selection buffer should yield an aptamer that is more sensitive and applicable to low millimolar concentrations of glucose in physiological conditions. Interestingly, glu1 and glu2 also showed a similar affinity to the parent aptamer when tested in HEPES buffer, with K_D values of 3.55 ± 0.51 and 3.74 ± 0.73 mM, respectively (Figure S5), showing that the mutations identified in the screen broadened the aptamer's effective operating conditions rather than yielding an aptamer that is solely optimized for use in selection buffer.

We used an equilibrium bead-based assay to evaluate glu1 and glu2 in real physiological conditions. Similar to the plate-reader assay, we measured the aptamer's ability to displace a 13-mer strand in response to glucose binding (Figure S6A). The biotinylated-aptamers were annealed with the Cy5-labeled displacement strand captured onto streptavidin T1 beads and then incorporated with target solution. The fluorescence signal was then measured on a flow cytometer and normalized using a no-target condition. Using the bead-based assay, we measured glu0, glu1, and glu2 in selection buffer and found that the three aptamers showed similar affinities to those measured in the plate-reader assay, demonstrating that the aptamers work comparably when bound to a surface (Figure S6B,C). As with before, glu1 and glu2 showed greater signal changes at low concentrations of glucose, whereas glu0 did not have significant signal differences (Figure 4). We similarly measured glu0, glu1, and glu2 in 80% filtered human serum with additional spiked glucose (Figure 4). Our top-performing double mutants glu1 and glu2 had 1.7 and 2.4% signal increases in the 1 mM spiked glucose over the serum-only condition, whereas glu0 had a 0.49% signal change. Both glu1 and glu2 show a significant signal change at low concentrations. Through the two-sample *t*-test, glu1 and glu2 have p-values of 0.0046 and 0.011, respectively, and are able to distinguish between 0 and 1 mM spiked glucose. In contrast, glu0 does show a significant signal difference, with a *p*-value of 0.14. Our top-performing double-mutant aptamer candidates could thus be usable in physiological conditions to measure relevant concentrations of glucose.

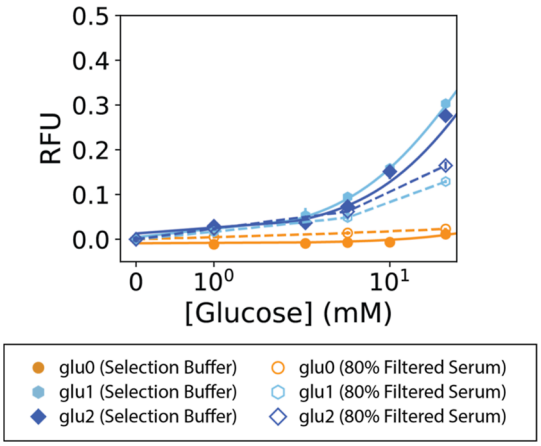

Figure 4. Measurement of low concentrations of glucose in physiological conditions. An equilibrium bead-based assay was used to measure glucose in physiological samples. The fluorescence was measured at various concentrations of glucose and normalized using the fluorescence with no glucose. The measurements were made in selection buffer and 80% filtered human serum. The measurements made in human serum are plotted at the spiked concentrations of glucose. At low (spiked) concentrations of glucose, the signal change is greater for glu1 and glu2 than for glu0.

CONCLUSIONS

In this work, we demonstrate a high-throughput screening strategy that allows us to identify mutant derivatives of an existing glucose aptamer that exhibit improved performance in a physiological buffer relative to the parent sequence, which was originally selected in a high ionic strength buffer. We screened nearly every possible single- and double-mutant of this aptamer for glucose binding in selection buffer using our N2A2 platform. While single-substitution mutants achieved a modestly improved response to glucose in selection buffer, we found that certain double mutations yielded synergistic improvements to affinity that allowed them to outperform any of the corresponding single mutants. The two top-performing double mutants, glu1 and glu2, exhibited a ∼four-fold improvement over the parent aptamer. Our analysis also yielded a mutation map that could be used to identify areas of the aptamer that might prove useful for further engineering of the aptamer. However, it is also worth noting that the impact of specific mutation combinations on the aptamer structure and function was not generally predictable, and this highlights the advantage of using a platform that can broadly screen large numbers of such mutants in a single experiment. We expect that our approach could be applied to other aptamers and environmental conditions to extend the utility of aptamers for a broader set of applications.

ASSOCIATED CONTENT

Supporting Information

The Supporting Information is available free of charge at https://pubs.acs.org/doi/10.1021/acssensors.2c02106.

https://doi.org/10.1021/acssensors.2c02106
ACS Sens. XXXX, XXX, XXX−XXX

Materials and methods; sequences used in the high-throughput mutational screen and in the plate reader characterization of sequences; measuring aptamer performance using a plate reader assay; identifying cooperative substitution mutations in the double mutant pool; non-cooperative single mutations; measuring the KD for glu1 and glu; KD of parent aptamer glu0 and mutants glu1 and glu2 in HEPES buffer; and bead-based assay for measurement of glucose in physiological conditions (PDF)

AUTHOR INFORMATION

Corresponding Author

H. Tom Soh − *Department of Radiology and Department of Electrical Engineering, Stanford University, Stanford, California 94305, United States;* orcid.org/0000-0001-9443-857X; Email: tsoh@stanford.edu

Authors

Leighton Wan − *Department of Bioengineering, Stanford University, Stanford, California 94305, United States;* orcid.org/0000-0001-8935-4144

Alex Yoshikawa − *Department of Radiology, Stanford University, Stanford, California 94305, United States*

Michael Eisenstein − *Department of Radiology and Department of Electrical Engineering, Stanford University, Stanford, California 94305, United States*

Complete contact information is available at: https://pubs.acs.org/10.1021/acssensors.2c02106

Funding

This work was supported by the W. L Gore & Associates, the Helmsley Trust, the Wellcome Leap SAVE program, the Stanford Pediatric Inflammatory Bowel and Celiac Disease Research Program, and the National Institutes of Health (NIH, OT2OD025342, and R01GM129314-01).

Notes

The authors declare no competing financial interest.

REFERENCES

(1) Tuerk, C.; Gold, L. Systematic Evolution of Ligands by Exponential Enrichment: RNA Ligands to Bacteriophage T4 DNA Polymerase. *Science* **1990**, *249*, 505−510.

(2) Ellington, A. D.; Szostak, J. W. In vitro selection of RNA molecules that bind specific ligands. *Nature* **1990**, *346*, 818−822.

(3) Edwards, K. A.; Wang, Y.; Baeumner, A. J. Aptamer sandwich assays: human α-thrombin detection using liposome enhancement. *Anal. Bioanal. Chem.* **2010**, *398*, 2645−2654.

(4) Witt, M.; Walter, J.-G.; Stahl, F. Aptamer Microarrays—Current Status and Future Prospects. *Microarrays* **2015**, *4*, 115−132.

(5) Reuss, A. J.; Vogel, M.; Weigand, J. E.; Suess, B.; Wachtveitl, J. Tetracycline Determines the Conformation of Its Aptamer at Physiological Magnesium Concentrations. *Biophys. J.* **2014**, *107*, 2962−2971.

(6) Carothers, J. M.; Goler, J. A.; Kapoor, Y.; Lara, L.; Keasling, J. D. Selecting RNA aptamers for synthetic biology: investigating magnesium dependence and predicting binding affinity. *Nucleic Acids Res.* **2010**, *38*, 2736−2747.

(7) Misra, V. K.; Draper, D. E. The linkage between magnesium binding and RNA folding. *J. Mol. Biol.* **2002**, *317*, 507−521.

(8) Nakatsuka, N.; Abendroth, J. M.; Yang, K.-A.; Andrews, A. M. Divalent Cation Dependence Enhances Dopamine Aptamer Biosensing. *ACS Appl. Mater. Interfaces* **2021**, *13*, 9425−9435.

(9) Neves, M. A. D.; Reinstein, O.; Saad, M.; Johnson, P. E. Defining the secondary structural requirements of a cocaine-binding aptamer by a thermodynamic and mutation study. *Biophys. Chem.* **2010**, *153*, 9−16.

(10) Wu, D.; Feagin, T.; Mage, P.; Rangel, A.; Wan, L.; Kong, D.; Li, A.; Coller, J.; Eisenstein, M.; Soh, H. Flow-Cell-Based Technology for Massively Parallel Characterization of Base-Modified DNA Aptamers. *Anal. Chem.* **2023**, *95*, 2645−2652.

(11) Yoshikawa, A. M.; Wan, L.; Zheng, L.; Eisenstein, M.; Soh, H. T. A system for multiplexed selection of aptamers with exquisite specificity without counterselection. *Proc. Natl. Acad. Sci. U.S.A.* **2022**, *119*, No. e2119945119.

(12) Nakatsuka, N.; Yang, K.-A.; Abendroth, J. M.; Cheung, K. M.; Xu, X.; Yang, H.; Zhao, C.; Zhu, B.; Rim, Y. S.; Yang, Y.; et al. Aptamer−field-effect transistors overcome Debye length limitations for small-molecule sensing. *Science* **2018**, *362*, 319−324.

(13) American Diabetes Association. Diagnosis and Classification of Diabetes Mellitus. *Diabetes Care* **2006**, *29*, S43−S48.

(14) Yang, K.-A.; Pei, R.; Stojanovic, M. N. In vitro selection and amplification protocols for isolation of aptameric sensors for small molecules. *Methods* **2016**, *106*, 58−65.

(15) Fornace, M. E.; Porubsky, N. J.; Pierce, N. A. A Unified Dynamic Programming Framework for the Analysis of Interacting Nucleic Acid Strands: Enhanced Models, Scalability, and Speed. *ACS Synth. Biol.* **2020**, *9*, 2665−2678.

https://doi.org/10.1021/acssensors.2c02106
ACS Sens. XXXX, XXX, XXX−XXX